Effect of Exothermic Interfacial Mixing on Interfacial Activity of a Block Copolymer

Adeyinka Adedeji, Steven D. Hudson,* and Alex M. Jamieson

Department of Macromolecular Science, Case Western Reserve University, Cleveland, Ohio 44106

Received August 31, 1995; Revised Manuscript Received January 22, 1996[⊗]

ABSTRACT: Variation in the enthalpic interaction of a block copolymer (bcp) at the phase boundary between immiscible homopolymers is demonstrated to strongly modulate the critical micelle concentration, the interfacial activity, and the emulsifying power, by tracing morphological transformations using transmission electron microscopy (TEM). Moreover, the theory of micellization by Leibler et al. is modified to account for such interaction. Specifically, it is demonstrated that, while incompatibility between a bcp segment and a homopolymer drives the bcp to the interface (increases interfacial activity), exothermic mixing reduces interfacial activity. However, when the bcp is interfacially active, exothermic mixing can enhance interfacial wetting (emulsifying power). In addition, we show that too strong a swelling of an interfacially-active bcp block by the major blend component can cause a reduction in emulsifying power. Solution-cast blends of poly(styrene-*co*-acrylonitrile) (SAN) with polystyrene (PS) as a minor component and emulsified with poly(methyl methacrylate-*b*-styrene) (PMMA-*b*-PS) were investigated. Three molecular weights of PMMA-*b*-PS (65, 283, and 680 kDa) were used. The exothermic mixing between SAN and PMMA and the repulsion between SAN and PS were systematically varied by changing the AN content of the SAN from 15 to 26, 29, and 33%. We find that the degree of incompatibility $N\chi_{SAN-PS}$, the molecular weight ratio M_h/M_b of PS homopolymer to PS bcp segment, and the degree of exothermic mixing between SAN and PMMA are all important in determining the morphology of the disperse phase.

Introduction

Block copolymers (A-*b*-B) with immiscible segments A and B exhibit properties analogous to those of low molar mass surfactants. For example, they exhibit microphase separation to form morphological structures which minimize the unfavorable contacts and the interfacial curvature energy.[1,2] Different micellar morphologies (spherical, cylindrical, lamellar) can be obtained[3−11] in binary bcp/homopolymer mixtures, by varying the molecular weight of the bcp, the relative length of block A to that of B, the relative molecular weight of the homopolymer (M_{hA} or M_{hB}) to that of the corresponding block segment, the bcp volume (or weight) composition, and the enthalpic interaction between the homopolymer and the bcp. Such microstructures in binary bcp/homopolymer mixtures are the result of macromolecular self-association when the concentration of bcp exceeds the critical micellar concentration (cmc) i.e., the concentration at which micelle formation is initiated in the bulk homopolymer.[12−14] Leibler et al.[12] have shown theoretically that the cmc depends on the degree of incompatibility $N\chi_{AB}$ (where $N = N_A N_B/(N_A^{1/2} + N_B^{1/2})^2$ is the effective degree of polymerization and χ_{AB} is the Flory−Huggins parameter which describes the repulsion between monomers A and B): when $N\chi_{AB}$ increases, there is a stronger driving force for chains to aggregate into micelles to lower the interaction energy; hence the cmc decreases.

When block B is the minor phase, the interfacial region which contains homopolymer A solubilized in block A is referred to as the corona and surrounds the micellar interior that accommodates the B segment (called the core). The degree of solubilization of homopolymer A in block A influences the coronal volume. The volume of the corona relative to that of the core determines the interfacial curvature or the shape of the micelle.[3−14] Structural transformations can thus be induced by changing the corona volume through changes in the solubility of matrix polymer in the corona. Homopolymer A entropically solubilizes in block segment A only when molecular weight of the homopolymer A is equal or lower than that of block A, i.e., when M_{hA}/M_{bA} is less than or equal to unity.[3−14] However, maximal corona swelling is limited by M_{bA} and the maximum extent to which block A can be stretched before a reduction in entropy sets in. The latter is described as elastic or turning back entropy.[12−16] In addition, swelling of block A occurs both axially (normal to the interface) and laterally (parallel to the interface). This leads to an increase in the area per copolymer junction. The spatial expansion of block A chains induces a decrease in the core volume as the core chains rearrange to maintain a constant density: the core chains are therefore axially contracted but laterally elongated.[6,7] Figure 1 shows a schematic illustration of the configuration of block copolymer chains in the core and in the corona, and the arrows indicate the directions of chain expansion or contraction.

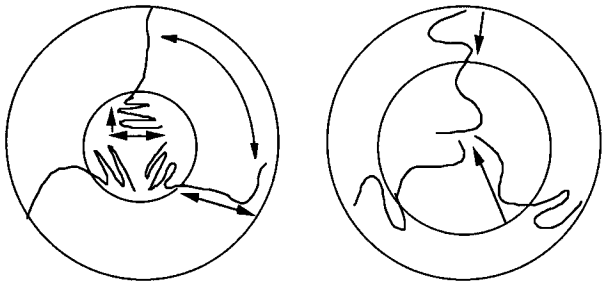

Figure 1. Schematic illustration of (a) strong coronal swelling leading to axial and lateral extension of the block copolymer chains in the corona which induces lateral extension and axial contraction of the core chains and small core volume; (b) weak coronal swelling with lateral extension of the core chains leading to larger core volume.

When two homopolymers A and B are immiscible, they exhibit high interfacial tension, which leads to stable disperse-phase particles of large size and wide

[⊗] Abstract published in *Advance ACS Abstracts,* March 1, 1996.

0024-9297/96/2229-2449$12.00/0

size distribution. A common remedy is to add a small quantity of bcp (A-*b*-B) to lower the interfacial tension and prevent coalescence, by localizing at the boundary between the phases A and B.[17] However, Leibler[14] has pointed out that the exponential decrease in $\Delta\gamma$ occurs only at very small copolymer contents, until the cmc is reached in one bulk phase, subsequent to which $\Delta\gamma$ does not change on further increase in bcp concentration. A longer bcp saturates the interface at a lower concentration; i.e., it has a lower cmc beyond which the bcp chains start to form micelles in the bulk homopolymers.[14−16] However, although fewer chains of a large bcp are required to saturate the interface, if the molecular weight is too large, a kinetic effect retards their diffusion to the interface, and instead they form micelles.[14−16] This imposes an upper bound on molecular weight of a bcp for interfacial activity. On the other hand, as noted above, if the molecular weights of the bcp segments are lower than those of the homopolymers in A/A-*b*-B/B blends, the bcp segments will not be solubilized by the matrix homopolymers.[3−14] This, imposes a lower bound on molecular weight of a bcp for interfacial activity. Hence, there is a bcp molecular weight window for optimal interfacial activity.

Theoretically, the interfacial activity or the cmc has not been studied when one or more of the bcp segments has an exothermic or attractive interaction with the matrix polymers. However, qualitatively, a new behavior may be expected to occur. If the attraction strongly offsets the repulsive forces which drives the bcp to the interface, the bcp will become dissolved or form micelles in the more compatible of the homopolymers. Clearly, in such blends, the role of the enthalpic interactions must be carefully considered in designing an interfacially-active bcp. In the present investigation, we examine the relative roles of enthalpic attraction (negative χ) and repulsion ($N\chi$, where χ is positive) in contributing to the interfacial activity of a bcp in a model blend A/X-*b*-B/B, where $\chi_{AX} < 0$, but χ_{AB} and $\chi_{BX} > 0$.

Akiyama and Jamieson[18] and Siqueira and Nunes[19] have demonstrated morphological transformations in blends of the type A/X-*b*-B/B, where exothermic mixing occurs on only one side of the interface, i.e., between A and X. Of particular interest here is the investigation by Akiyama and Jamieson[18] in which morphological transformations in ternary polystyrene/poly(styrene-*b*-methyl methacrylate)/poly(styrene-*co*-acrylonitrile) blends (i.e., PS/PS-*b*-PMMA/SAN) and also in binary SAN/PMMA-*b*-PS blends, with PS as the minor phase, were produced by systematically varying the degree of exothermic mixing between SAN and PMMA as well as the repulsion between SAN and PS. This was accomplished by changing the acrylonitrile (AN) content of the SAN from 15 to 26, to 29, and to 33%.[20,21] A 40:60 PMMA-*b*-PS diblock copolymer was used which had a M_w of 305 kDa, $M_{hPS}/M_{bPS} = 0.33$, and $M_{hSAN}/M_{hPMMA} = 0.62$, where M_h = molecular weight of homopolymer and M_b = molecular weight of block segment. At 15% AN content, where exothermic mixing of SAN/PMMA is greatest, the corona is maximally swollen, and small, spherical PS micelles were observed.[18] Larger spherical micelles were found when the AN content was 26% (SAN26). On further increasing the AN content to 29 and 33% (SAN29 and SAN33), with a corresponding decrease in the SAN/PMMA exothermic interaction, the micellar structure transformed to vesicles and cylinders interpreted as due to a reduction of the corona thickness.[18] Furthermore, Akiyama and Jamieson[18] reported that the PMMA block could be specifically stained only in blends containing SAN29 and SAN33, indicative that the PMMA block chains are less swollen, the corona volume is small, and hence the interfacial PMMA concentration is higher. These observations demonstrate, in agreement with independent studies,[22−27] that an exothermic interaction acts as an additional driving force for mixing of homopolymer B (or SAN) with block X (or PMMA segment), thereby increasing the corona volume and enhancing the emulsifying ability of the bcp.

Table 1. Characteristics of Polymer Blend Components

abbrev	acrylonitrile content (%)	M_w ($\times 10^{-3}$)	M_w/M_n	wt ratio (PMMA:PS)
PS		90[a]	1.04	
SAN15	15	163[b]	2.12	
SAN26	26	153[b]	2.16	
SAN29	29	151[b]	2.23	
SAN33	33	130[b]	1.95	
B(65)		65.5[c]	1.06	32500:33000
B(283)		283.4[d]	1.09	163000:120400
B(680)		680[c]	1.10	220000:460000

[a] Purchased from Pressure Chemical Co., lot no. 50522. [b] Determined by light scattering;[31] supplied by Mitsui Toatsu Chemicals Inc. [c] Purchased from Polysciences Inc. [d] Purchased from Polymer Laboratories Inc.

In the present study, we investigate the effect of PMMA-*b*-PS molecular weight on its interfacial activity in both binary SAN/PMMA-*b*-PS and ternary SAN/PMMA-*b*-PS/PS blends at different degrees of enthalpic interaction, obtained by varying the AN content of the SAN from 15 to 26, 29, and 33%. The magnitude of the repulsion between the bcp and the matrix homopolymer(s), i.e., the degree of incompatibility, will be characterized by $N\chi_{SAN-PS}$, where $N = N_{SAN}N_{bPS}/(N_{SAN}^{1/2} + N_{bPS}^{1/2})^2$ is the effective degree of polymerization, and χ_{SAN-PS} is the repulsive SAN/PS interaction. Hence the degree of incompatibility can be modulated by varying both the molecular weight of the bcp and the AN content of the SAN. The entropic contribution to the interfacial swelling or the emulsifying power of the bcp will be recognized by indicating for each blend the M_h/M_b ratios. Specifically, we seek to discover if there are particular values of $N\chi_{SAN-PS}$ that are optimal for a bcp to be interfacially active in the presence of exothermic mixing, and if a bcp is interfacially active, we want to further demonstrate how the degree of exothermic mixing influences its emulsifying power as manifested by changes in microstructure formation. Moreover, we extend the theoretical description of the cmc by Leibler et al.[12] to A/X-*b*-B blends.

Experimental Section

Materials. Characteristics of the polymers utilized in this study are presented in Table 1 together with their respective sources. The SANs will be referred to, henceforth, as SAN15, SAN26, SAN29, and SAN33, where the last two digits indicate the percentage AN content. The block copolymers and the PS homopolymers are standard polymers and were used as supplied without further purification. Numerical values of ratios of the molecular weights of the homopolymers to those of the compatible block segments (M_h/M_b) are presented in Table 2. There are only small changes in M_h/M_b when comparing the various SAN copolymers from SAN15 to SAN33; therefore, in evaluating the effect of AN content on emulsifying power of the block copolymer in this and in our earlier studies,[18] the dominant contribution is due to the change in enthalpic interactions. Note that by varying only the molecular weight of the block copolymer, we can systematically study the effect of changes in $N\chi_{SAN-PS}$ on the morphological characteristics of the blends.

Table 2. Ratios of Molecular Weights of the Matrix Polymers to That of the Compatible Block Copolymer Segment (M_h/M_b) in the Ternary Blends

abbrev	PS M_h/M_b	SAN15 M_h/M_b	SAN26 M_h/M_b	SAN29 M_h/M_b	SAN33 M_h/M_b
B(65)	2.7	5.02	4.71	4.65	4.0
B(283)	0.75	1.0	0.94	0.93	0.80
B(680)	0.20	0.74	0.70	0.67	0.59

Sample Preparation. Stock solutions of these polymers were made up in methyl ethyl ketone (MEK) solvent at a concentration of 1 g/100 mL. Each binary blend contains 80 v/v % of the SAN solution and 20% of one PMMA-*b*-PS solution. And each ternary blend contains 77.5 v/v % of SAN, 15 v/v % of one PMMA-*b*-PS, and 7.5 v/v % of PS, except when otherwise stated. The blend solutions were cast on a clean mercury surface, in hollow test tubes, and the solvent was slowly removed at room temperature over 7 days. Final traces of the solvent were removed by drying at 70 °C for 1 day at atmospheric pressure and then for 1 day under vacuum. The samples were further annealed at 105 °C (above the highest T_g) for 5 days.

Transmission Electron Microscopy. Central portions of the cast films (~0.2−0.4 mm thick) were sectioned, using a diamond knife, with a RMC Inc. MT-7000 microtome machine in a direction normal to the surface to obtain thin films (70−90 nm thick). These were subsequently exposed to RuO_4 vapor for 45 min in an enclosed chamber containing 1.5% aqueous solution of RuO_4. The PS component in the specimen is stained with the RuO_4. Bright-field images were obtained by mass−thickness contrast on a JEOL JEM-100SX transmission electron microscope at 100 kV. The PS minor phase appears as the darkest regions in the TEM micrographs since PMMA and the SANs are only lightly stained.

Results and Discussion

Binary Blends. The electron micrographs of the binary blends containing 20% bcp B(680) mixed with 80% SAN are displayed in Figure 2. In the blends containing SAN15 and SAN26 (Figure 2a,b, respectively), no micelles can be seen. Instead we observe only concentration fluctuations of the bcp PS segment as indicated by the irregularly-shaped dark areas in the micrographs. This is attributable to the comparatively weak SAN15/PS and SAN26/PS repulsion and the strong exothermic SAN15/PMMA and SAN26/PMMA mixing. However, in blends containing SAN29 and SAN33 as evident in Figure 2c,d, respectively, on increasing the SAN/PS repulsion and decreasing the SAN/PMMA attraction, formation of discrete micelles of B(680) is observed. The absence of micelles in SAN15/B(680) and SAN26/B(680) blends shows that the SAN/PMMA exothermic mixing dramatically increases the cmc. When the SAN/PS incompatibility is increased, coupled with a weaker SAN/PMMA exothermicity, as in the SAN29 and SAN33 blends, micelles are indeed produced (Figure 2c,d). We note that the average size of the micelles in Figure 2c,d is ~70 nm, which appears reasonable if we consider that the rms end-to-end distance of the PS segment of B(680) is estimated to be 46 nm, assuming a Gaussian coil.[28] It is pertinent to point out that in an earlier study[18] it was found that micelles are formed at all levels of AN content in SAN/B(305) blends containing 50% of B(305); i.e., the cmc in SAN15/B(305) blends is below 50%.[18] These experiments, as well as morphological deduction made from consideration of the appearance of the SAN-rich phase in the ternary SAN/B(65)/PS blend systems, are summarized in Table 4.

To provide a theoretical context to discuss these results, the model of Leibler et al. (LOW)[12] is extended

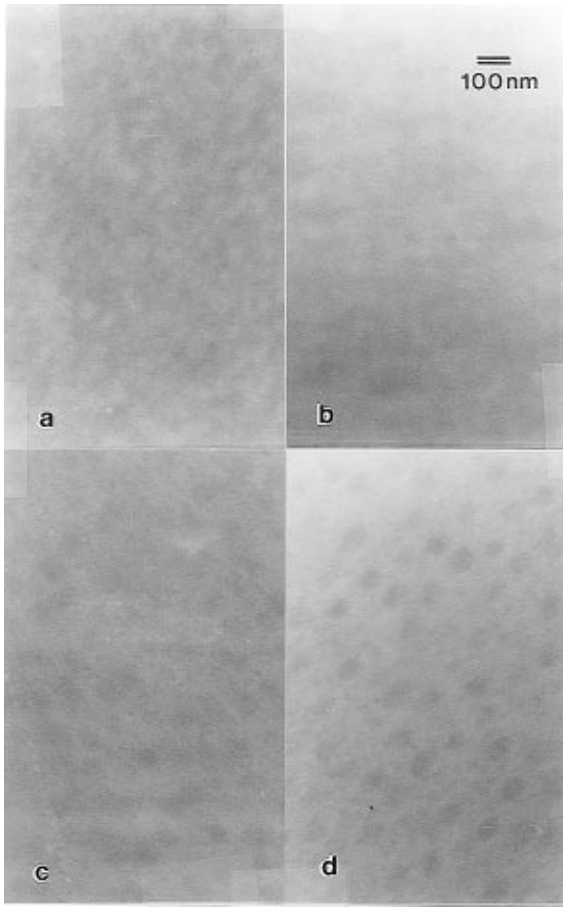

Figure 2. Morphology of SAN/B(680) binary blends: (a) SAN15; (b) SAN26; (c) SAN29; (d) SAN33. Only concentrations fluctuations of the PS segment of the B(680) dissolved in the SAN are observed in SAN15 and SAN26 blends, but a microphase is formed as the SAN/PS repulsion increases in SAN29 and SAN33 blends. Each blend contains 80% SAN and 20% PMMA-*b*-PS(680 kDa).

Table 3. Degree of Incompatibility of the PS Block Segments by the SAN Matrices Characterized by $N\chi$, Where $N = N_{SAN}N_{bPS}/(N_{SAN}^{1/2} + N_{bPS}^{1/2})^2$, for Unsymmetric Polymer Pairs[a]

X	χ_{X-PS} (cal/cm^3)	B(65) $N\chi_{X-PS}$	B(283) $N\chi_{X-PS}$	B(680) $N\chi_{X-PS}$
SAN15	0.169	26	58	107
SAN26	0.293	45	100	185
SAN29	0.327	50	112	207
SAN33	0.372	57	127	235
PMMA	0.040	5	10	12

[a] χ is calculated using the molar volume of styrene.

to include exothermic interaction. We consider a block copolymer, X-*b*-Y, mixed with a homopolymer A. The respective degrees of polymerization of each chain are N_X, N_Y, and N_A. The statistical segments of each are assumed to be equal, of length a and volume a^3. It is convenient to make the following identities: $N_X + N_Y = N$, $g = N_Y/N$, and $\alpha = N/N_A$. Repulsion between X and Y chains and A and Y chains leads to the formation of micelles, having a core comprising Y chains and having radius R_Y. R_X is the radius (thickness) of the corona, and R is the total radius. The concentration of X chains, η, in the corona is assumed constant; the volume fraction of A chains in the corona is $1 - \eta$. The repulsive interaction parameters, χ_{XY} and χ_{YA}, are assumed equal. Moreover, the micelles are assumed to be monodisperse, each having a number, p, of bcp chains per micelle.

Table 4. Incompatibility and Compatibility Parameters for Binary Blends

	copolymer B(65)			copolymer B(680)		
A	N_S 320 $\chi_{AS}N_S$	N_M 320 $\chi_{AM}N_M$	micelles?	N_S 4600 $\chi_{AS}N_S$	N_M 2200 $\chi_{AM}N_M$	micelles?
SAN15	54	−5	no	777	−33	no
SAN26	9	−3	yes	1350	−22	no
SAN29	105	−2	yes	1500	−11	yes
SAN33	119	−1	yes	1710	−4	yes
PMMA,M_w = 24K	13	0	yes	184	0	yes

Following LOW, the free energy of a micelle is the sum of the interfacial, chain distortion, and corona mixing free energies.

$$F = F_i + F_d + F_m \tag{1}$$

The entropic effect of localization of the copolymer junction is neglected as in LOW. Block asymmetry, g, modifies each of the above terms, but the additional enthalpic interaction in the corona changes only the corona mixing free energy, F_m:

$$F_i/kT = A_1'\chi_{XY}^{1/2}(gpN)^{2/3} \tag{2a}$$

where $A_1' = 6^{1/6}\pi^{1/3} = A_1 2^{2/3}$, where A_1 is as given in LOW

$$F_d/kT = A_2'(1 + C'\leq g/(1-g))p^{5/3}g^{-1/3}N^{-1/3} + A_3'(1 + (1-g)/(C'g))p^{1/3}g^{1/3}N^{1/3} - 6p \tag{2b}$$

where $A_2' = 3^{5/3}2^{-7/3}\pi^{-2/3} = A_2 2^{-1/3}$, $A_3' = 3^{1/3}2^{1/3}\pi^{-2/3} = A_3 2^{1/3}$, and $C' = [(1 + (1-g)/(\eta g))^{1/3} - 1]^2$, where A_2 and A_3 are as given in LOW and C' is the modified LOW C.

$$F_m/kT = p(1-g)\alpha(1-\eta)/\eta \ln[1-\eta] + \chi_{XA}N_X(1-\eta)p \tag{2c}$$

The original LOW expressions are recovered if one sets $g = 0.5$ and $\chi_{XA} = 0$. The free energy per copolymer chain is written as kTf, where

$$f = A_1'\chi_{XY}^{1/2}(gN)^{2/3}p^{-1/3} + A_2'(1 + C'g/(1-g))p^{2/3}g^{-1/3}N^{-1/3} + A_3'(1 + (1-g)/C'g)p^{-2/3}g^{1/3}N^{1/3} - 6 + (1-g)\alpha(1-\eta)/\eta \ln[1-\eta] + \chi_{XA}(1-g)N(1-\eta) \tag{3}$$

which we will express as

$$f = f_0 + \chi_{XA}(1-g)N(1-\eta) \tag{4}$$

The total micelle free energy, $F/kT = pf$, is then compared to that for dissolved chains, where the overall concentration of bcp is ϕ

$$F_h/kT = \Omega\{(\phi/N)\ln\phi + ((1-\phi)\alpha/N)\ln[1-\phi] + \chi_{XY}g\phi(1-g\phi) + \chi_{XA}\phi(1-g)(1-\phi)\} \tag{5}$$

For any real mixture, there may be some fraction, ζ, of bcp chains in micelles and some concentration, ϕ_1, of free chains dissolved in the homopolymer A. The total free energy, $F_M/\Omega kT$, is the sum of three terms: (1) f times the fraction of bcp chains in micelles, (2) $F_h(\phi_1)$, where both ϕ_1 and F_h are calculated with consideration for the excluded volume of the micelles, and (3) the free energy arising from the translational entropy of the micelles.

Following LOW, the critical micelle concentration is calculated by minimizing the total free energy with respect to p, η, and the concentration of free bcp chains. Assuming, as did LOW, high incompatibility and a large number of chains per micelle, the critical micelle concentration is given as

$$\phi_{cmc} \sim \exp[-\chi_{XY}N_Y - \chi_{XA}N_X\eta + \alpha - 1 + f_0] \tag{6}$$

Equation 6 shows that, if χ_{XA} is negative, the "compatibility term" $\chi_{XA}N_X$ counteracts the "incompatibility term", $\chi_{XY}N$. Thus, one can design N_X and N_Y so that ϕ_{cmc} is large. Large ϕ_{cmc} can lead to emulsification failure as we describe experimentally below, because the bcp X-*b*-Y is drawn away from the A/B interface into the favorable domain, being found as either free chains or micelles. The interfacial activity can be increased if the swellings of X by A and Y by B are balanced.

Experimental results have already shown that the predictions of LOW are qualitatively, but not quantitatively, correct. In general, the experimental findings for ϕ_{cmc} are one or two orders of magnitude greater than the prediction. One important factor is the assumption that the interface between core and corona is sharp. If finite interfacial width is considered, the increase in unfavorable segmental contacts within a micelle increases f_0, which offsets the incompatibility term, thus raising the cmc. Such a reduction of the influence of the incompatibility term may explain our experimental results (Figure 2) which indicate a disproportionately large contribution from the compatibility term, $\chi_{XA}N_X\eta$.

In Table 4, we list the numerical value of the incompatibility parameters, $N_S\chi_{AS}$ and $N_M\chi_{AM}$, respectively, for each blend. Here, χ_{AS} is the interaction between the SAN matrix and the styrene block, and χ_{AM} is the interaction between the SAN matrix and the methyl methacrylate block. For comparison, we show an example where the matrix A is PMMA, allowing a comparison when the interaction χ_{AM} is zero. Clearly, the trend in $\chi_{AS}N_S$ and $\chi_{AM}N_M$ are qualitatively consistent with the morphological observations. However, one observes that the incompatibility term, $\chi_{AS}N_S$, is large compared to the compatibility term, $\chi_{AM}N_M$. The relative importance of the latter is evident by this comparison. For example, the high molecular weight copolymer is miscible with SAN26, whereas it forms micelles in PMMA, even though the incompatibility term is much smaller in the latter case. It was argued above that the incompatibility term may be strongly offset by the parameter f_0.

Ternary Blends. SAN/B(65)/PS. In these blends, as seen in Table 2, the ratio M_h/M_b of homopolymer molecular weight to that of the miscible block is substantially larger than unity in both the SAN/PMMA and PS/PS phases, so that the entropic driving force for solubilization of the copolymer is minimal. As evident in Figure 3a−d, we observe macrophase separation with large PS-rich domains in SAN-rich continuous matrices.

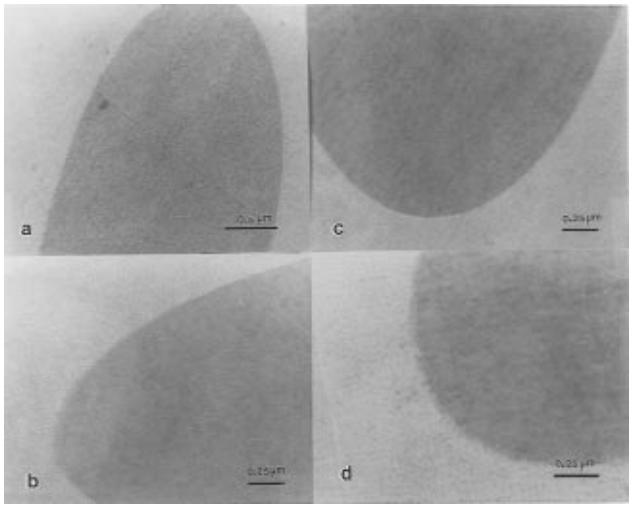

Figure 3. Morphology of SAN/B(65)/PS blends: macrodomains of PS homopolymer coexist with micelles of B(65) in the SAN matrix. (a) SAN15; (b) SAN26; (c) SAN29; (d) SAN33.

In these blends, it appears that all of the bcp is concentrated in the SAN phase, where it is present at a level of ~20%. Only the SAN phase provides an exothermic driving force for solubilization, and therefore the bcp is asymmetrically distributed. In the blend containing SAN15 (Figure 3a), the SAN15-rich matrix appears homogeneous, and the PS-rich phase does not show any secondary microstructures even at higher resolution. However, in blends containing SAN26, SAN29, and SAN33 (Figure 3b,d), there are micelles of B(65) bcp in the SAN-rich continuous phase. The diameter of these particles appears to be ~13.5 nm, which is to be compared with the value 12.3 nm estimated for the rms end-to-end distance of the PS block. Thus, there is no significant amount of PS homopolymer within the micelles.

The repulsion of the PS block by the PMMA block and by the SAN matrix coupled with that between the PS homopolymer and the PMMA block (characterized by $\chi_{PMMA-PS}$, χ_{SAN-PS}, and $\chi_{PMMA-PS}$, respectively) each provides a driving force for migration of the bcp to the interface. The dominant contribution comes from $N\chi_{SAN-PS}$ for the SANs and the PS block whose values are presented in Table 3. Clearly, Table 3 indicates that the tendency of the bcp to migrate to the interface is increased by increasing bcp molecular weight at fixed AN content and by increasing AN content at fixed block copolymer molecular weight. Since we observe PS-rich macrodomains in Figure 3a−d, this implies that migration of the bcp to the interface does not occur when $N\chi_{SAN-PS}$ is within the range of 26−57 at the chosen blend composition. The absence of microstructures within the PS-rich macrodomains in Figure 3a−d suggests that there is very little B(65) in the PS-rich phase. Thus the bcp is concentrated in the SAN matrix where, in SAN15, at maximal SAN−PMMA exothermic interaction it appears to be miscible, and at higher AN, it forms micellar structures. It should be noted that a small amount of PS must be dissolved within the core of the micelles, because the cmc is decreased in the ternary blend. Micelles are distinct in the ternary blend containing SAN26, whereas in the binary blend, having the same relative amounts of SAN26 and bcp, no micelles were present. Such influence of a third component on the cmc has been noted before for bcp solutions.[29]

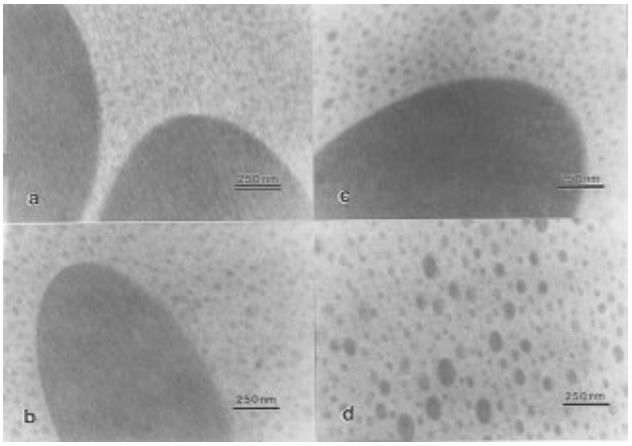

Figure 4. Morphology of SAN/B(283)/PS blends: (a) PS-rich macrodomains in the SAN-rich matrix in SAN15/B(283)/PS; (b) PS-rich macrodomains in the SAN-rich matrix in SAN26/B(283)/PS; (c) B(283) micelles and PS-rich macrodomains in SAN29/B(283)PS; (d) only B(283) micelles in SAN33/B(283)/PS.

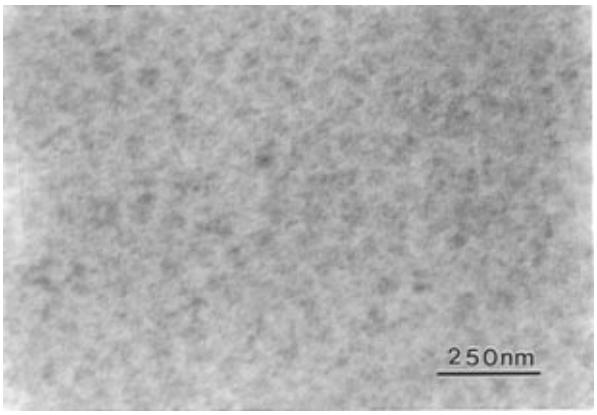

Figure 5. Microstructure of SAN15/B(283)PS blend on increasing the concentration of B(283) to 26.1%: only micelles are formed.

SAN/B(283)/PS. By increasing the block copolymer molecular weight, we decrease the M_h/M_b ratio below unity on the PS/PS side (see Table 2 for numerical values) while the molecular weights of SAN and PMMA segment become comparable ($M_h/M_b \sim 1$). Note that this coincides with the requirement for interfacial solubilization in A/A-*b*-B/B blends.[3−14] In addition, the effective degree of polymerization N increases, and hence $N\chi_{SAN-PS}$ and $N\chi_{PMMA-PS}$ each increase, which enhances the driving force for migration of the bcp to the interface each increase. Morphological behavior of these blends is presented in Figure 4a−d. The blend containing SAN15 shows PS-rich macrodomains in the SAN matrix (Figure 4a). As before, the copolymer is dissolved in the SAN; gray-level variations indicate fluctuations in the PS concentration from the solubilized B(283). In these blends, if we increase the concentration of the B(283) onset of micellization is expected. Indeed, when the B(283) concentration is increased from 15 to 26.1% (see Figure 5), the macrodomains disappear and only small sized micelles are observed. Note that in SAN15 blends the staining contrast between SAN and PS is poor relative to SANs with higher AN content.

In the blend containing SAN26 (Figure 4a), B(283) is solubilized in the SAN-rich matrix, and microdomains are clearly formed by mutual association of the B(283) chains. The PS microdomains are polydisperse with an average diameter of 39 nm. This is larger than the rms

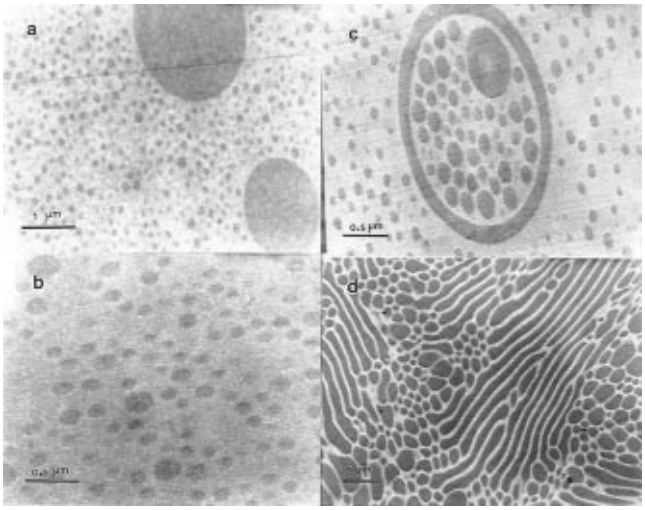

Figure 6. Microstructural transformation from spherical micelles to vesicles and cylinders as AN content increases from 15 to 33% in SAN/B(680)/PS blends with interfacially-active B(680): (a) spherical micelles coexisting with PS macrodomain in SAN15/B(680)/PS; (b) only spherical micelles in SAN26/B(680)/PS; (c) spherical micelles and vesicles in SAN29/B(680)/PS; (d) spherical and elongated micelles in SAN33/B(680)/PS.

end-to-end distance of the PS block anticipated[28] for micelles assuming that the configuration of the PS bcp segment is Gaussian, indicating that there is significant solubilization of homopolystyrene by the bcp. The PS-rich macrodomains again do not show any microstructures. Similar morphology is observed in the blend containing SAN29 (Figure 4c). Again, spherical micelles of the B(283) coexist with PS-rich macrodomains in the SAN29 matrix. The average micelle diameter is approximately the same as in the SAN26 blend (~39 nm). On further increasing the AN content to 33%, i.e., SAN33 (Figure 4d), we find only spherical micelles of the PS and a complete absence of PS-rich macrodomains. In addition, the average micelle diameter has increased to 53 nm. This indicates that the emulsifying power of B(283) is increased in the SAN33 blend, reflecting the higher degree of incompatibility between SAN33 and the PS block, coupled with poorer SAN33/PMMA exothermic mixing. Clearly, the systematic emergence of microphase in SAN/B(283)/PS blends can be attributed to an increase in the degree of SAN/PS incompatibility, $N\chi_{SAN-PS}$, and a decrease in SAN/PMMA exothermic mixing.

SAN/B(680)/PS. Further increment of the bcp molecular weight to 680 kDa results in a further decrease of the M_h/M_b ratio in both SAN/PMMA and PS/PS phases to values substantially below unity (see Table 2). In addition, $N\chi_{SAN-PS}$ and $N\chi_{PMMA-PS}$ are further increased, and the tendency of the bcp to migrate to the interface is likewise enhanced. As evident in the micrographs of these blends, displayed in Figure 6a−d, in increasing order of AN content, formation of microphase indicates that the bcp migrates to the SAN/PS interface at all SAN compositions and therefore gives us the opportunity to evaluate the contribution of exothermic mixing to the emulsifying power of an interfacially-active bcp. The results show that there is a systematic variation of the microstructures from spherical microdomains coexisting with macrophase (SAN15) to spherical microdomains only (SAN26), to spherical microdomains coexisting with a few vesicles (SAN29), and subsequently to coexisting spherical and elongated microdomains (SAN33). Note that these

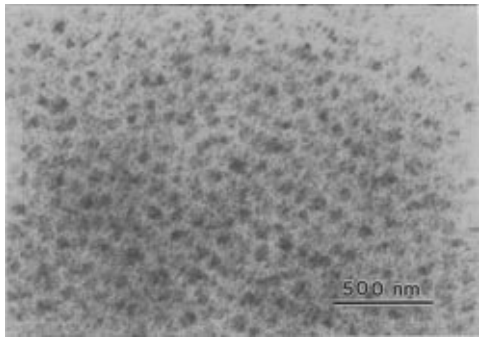

Figure 7. Microstructure of SAN15/B(680)/PS blend on increasing the concentration of B(680) from 15 to 26.1%: only micelles are formed and the size of the micelles is reduced.

variations are analogous to those reported in the earlier study of Akiyama and Jamieson.[18] However, in the present case, we have a smaller M_h/M_b ratio (=0.2) on the PS/PS side of the interface which enhances the dissolution of the PS segment, thereby increasing the swelling activities in the microdomain interior. This is partially offset by the fact that M_h/M_b for SAN/PMMA is smaller than in the earlier study[18] and ranges between 0.59 and 0.74.

In the blend containing SAN15 (Figure 6a), where the exothermic interaction between SAN and PMMA is maximal, small spherical microdomains containing the PS component coexist with PS-rich macrodomains. This phenomenon of coexistence of a microemulsion with a discrete phase of excess minor component is referred to by Wang and Safran[1] as "emulsification failure" and is due to an insufficient quantity of bcp to fully emulsify the immiscible blend.[1] Thus, an increment in the B(680) concentration is expected to reduce the size of the PS-rich macrodomains. Indeed, as shown in Figure 7, when the B(680) content is increased from 15 to 26.1%, we observe only micelles with a complete absence of macrodomains. Furthermore, when the concentration of the bcp is lowered to 7.5%, more macrodomains and fewer microdomains appeared (micrograph not shown). The surface curvature of the spherical micelles (or microemulsion) in blends containing SAN15 is expected to be very high as a result of the strong exothermic mixing between SAN15 and PMMA. This results in a large extension of the PMMA block and produces a large corona volume. Thus, spherical micelles of high interfacial curvature and small radius are formed. Because of the concomitant increase in interfacial area, more bcp is required to fully emulsify the blend, hence the presence of PS macrodomains.

When the AN content is increased to 26%, i.e., SAN26, leading to a decrease in the SAN/PMMA exothermic mixing coupled with an increase in the $N\chi_{SAN-PS}$, only spherical micelles are observed (Figure 7b). There are no PS-rich macrodomains as observed in the SAN15 blend. As previously discussed (see Figure 1), swelling of a block copolymer occurs both laterally and axially, leading to a decrease in the core chain density, and the chains in the core adjust in a fashion that will decrease the core volume so as to maintain a constant core chain density.[6,7] Since swelling of the PMMA block is lower in SAN26 than in SAN15, the core volume reduction in the SAN26 blend is smaller than in the SAN15 blend; therefore, the average diameter (160 nm) of the micelles in the SAN26 blend is larger than that in the SAN15 blend (140 nm). Likewise, $N\chi_{SAN-PS}$ is higher in SAN26, which increases the extension of the PS block segment in the core, again leading to an increase in the core

volume (see Figure 1b). The rms end-to-end distance of the PS block segment of B(680) is estimated to be 46 nm assuming a Gaussian coil.[28] When this value is contrasted with the experimental domain diameters of 140 and 160 nm in Figure 6a,b, respectively, it is clearly evident that the microdomains in the SAN15 and SAN26 blends contain some PS homopolymer. This is further support that the presence of macrophase in the SAN15 blend is an example of "emulsification failure" as described by Wang and Safran.[1]

In addition, measurement of the area occupied by a bcp chain at the interface (Σ) of a discrete spherical domain can be applied to probe the degree of swelling of the PMMA blocks in the corona. Σ can be estimated from a relationship suggested by Paul and Newman,[17] which we reformulate as

$$\Sigma = 3\Phi_A M/(\Phi_{bcp}\rho_{bcp} R N_A) \quad (7)$$

where Φ_A is the volume fraction of the minor blend component (A) that forms discrete spherical domains, ρ_{bcp} is the average bulk density of the bcp, M is the molecular weight of the bcp, Φ_{bcp} is the ratio of the volume of the bcp to the original volume of the blend, R is the radius of the spherical domain, and N_A is Avogadro's number. Using an average particle diameter of 140 nm for the microphase domains (Figure 6a) in the blend containing 77.5/7.5 of SAN15/PS with 15% bcp, eq 7 gives $\Sigma = 25$ nm^2; using an average particle diameter of 160 nm in the SAN26/PS blend, we obtain $\Sigma = 21$ nm^2, while the largest particles in the blend whose diameter is 286 nm yield $\Sigma = 11.5$ nm^2. These areas are all higher than the minimum value of $\Sigma = 0.5$ nm^2 corresponding to fully-stretched chains, as suggested by Paul and Newman,[17] and also greater than the value ($\Sigma = 10.6$ nm^2) estimated by Perrin and Prud'homme[30] from scanning microscopic images of a PS(30%)/PMMA(70%) blend. These values are also greater than $\Sigma = 9.95$ nm^2 determined by Russell et al.[31] using the neutron reflectivity technique to probe a PS/PMMA interface. This suggests that the block copolymer chains are configurationally more expanded in our exothermic blends compared to the athermal PS/PS-*b*-PMMA/PMMA.[30,31] This observation is conceptually in agreement with the schematic representation displayed in Figure 1. Note that similar morphologies are observed in Figures 4c,d and 6a,b. This is consistent with the fact that similar $N\chi_{SAN-PS}$ values are present for these blend pairs (cf. Table 3). To confirm the presence of PS homopolymer in the micelles, it would be advantageous to compare the domain sizes in the ternary SAN15/B(680)/PS(90) blend with those in the absence of PS(90) homopolymer, i.e., in the binary SAN15/B(680) blend (Figure 2a). Unfortunately, micelles are not formed in the binary blends. However, we note that the mean micellar size in the SAN29/B(680) and SAN33/B(680) blends (Figure 3c,d) is 70 nm, i.e., substantially smaller than the microdomain sizes in the ternary blends containing B(680).

On increasing the AN content to 29% (SAN29), there is a further decrease in the SAN/PMMA exothermic mixing and an increase in $N\chi_{SAN-PS}$. The reduction in the SAN/PMMA exothermic mixing leads to a decrease in the extension of the PMMA segment into the SAN matrix and, hence, a reduction of the corona volume. The increase in the SAN/PS repulsion coupled with the entropic PS/PS mixing enhances the swelling on the PS/PS side of the interface and results in an increase in the core volume. When the ratio of the SAN/PMMA corona volume to that of the PS/PS core decreases, the interfacial curvature is expected to decrease and the minor component starts to show vesicular structure as seen in Figure 6c. The micelles are predominantly spherical with few vesicles. When the AN content of the SAN is again increased to 33% (SAN33), the SAN/PMMA exothermic mixing is further decreased and the $N\chi_{SAN-PS}$ is similarly increased. The corona volume is further decreased while the core volume increases. The ratio of the corona volume to that of the core becomes lower than in the SAN29 blend, leading to a further reduction of the interfacial curvature and formation of elongated micelles as observed in Figure 6d.

Conclusions

Morphological studies in binary SAN/PS-*b*-PMMA blends have generated experimental evidence that the critical micellar concentration increases with increase in the exothermic interaction between SAN and PMMA and decrease in the endothermic interaction between SAN and PS (Figure 3). These results are consistent with theoretical analysis based on an extension of the LOW model. In ternary SAN/PS-*b*-PMMA/PS blends, with PS as the minor phase, there is a clear trend toward enhanced interfacial activity as the degree of SAN−PS incompatibility, $N\chi_{SAN-PS}$, increases, as the SAN−PMMA attraction decreases and the molecular weight ratios M_{hPS}/M_{bPS} and M_{hSAN}/M_{bPMMA} of compatible matrix polymer to corresponding block segment decrease. Thus, for the blends containing bcp of lowest molecular weight (B(65)), where $N\chi_{SAN-PS} = 26-57$ and $M_{hSAN}/M_{bPMMA} > M_{hPS}/M_{bPS} \gg 1.0$, there appears to be essentially complete rejection of bcp by PS macrophase into the SAN matrix where it dispersed molecularly or in the form of small micelles. At intermediate bcp molecular weigh (B(283)), where $N\chi_{SAN-PS} = 58-127$ and $M_{hPS}/M_{bPS} \leq M_{hSAN}/M_{bPMMA} \sim 1.0$, we see a trend from coexistence of PS macrophase with microphase in SAN15 to only microphase formation in SAN33 with a corresponding increase in microdomain sizes. At highest bcp molecular weight (B(680)), where $N\chi_{SAN-PS} = 107-235$ and $M_{hPS}/M_{bPS} \ll M_{hSAN}/M_{bPMMA} \leq 1.0$, we again see a systematic morphological variation from coexistence of PS macrodomains with microdomains in SAN15 to microdomains only in SAN26, SAN29, and SAN33. In addition, in the latter blends, there is a gradual trend toward more planar microdomain interfaces with increasing AN content of SAN. This is consistent with the earlier results of Akiyama and Jamieson.[18] For a bcp of specified molecular weight, these morphological patterns are clearly due to the shift in enthalpic interaction produced by varying the AN content of the SAN. In particular, the coexistence of PS macrodomains and microdomains in blends with a stronger exothermic interaction is an example of emulsification failure due to a too large swelling of the PMMA micellar corona relative to the PS micellar core. This decreases microdomain sizes and weakens the emulsifying power of the bcp. Finally, when the swelling in the micellar core is also very strong, a decrease in the degree of exothermic PMMA−SAN mixing coupled to an increase in the PS−SAN repulsion leads to formation of more planar interfaces in the microphase domains.

Acknowledgment. This work was supported by the National Science Foundation through Materials Research Group award DMR 01845.

References and Notes

(1) Wang, Z. G.; Safran, S. A. *J. Phys. (Paris)* **1990**, *51*, 185.
(2) Wang, Z. G.; Safran, S. A. *Europhys. Lett.* **1990**, *11*, 4253.
(3) Mayes, A. M.; Olvera de la Cruz, M. *Macromolecules* **1988**, *21*, 2543−2547.
(4) Kinning, D. J.; Winey, K. I.; Thomas, E. L. *Macromolecules* **1988**, *21*, 3502−3506.
(5) Kinning, D. J.; Thomas, E. L.; Fetters, L. J. *J. Chem. Phys.* **1989**, *90* (10), 5806−5825.
(6) Winey, K. I.; Thomas, E. L.; Fetters, L. J. *Macromolecules* **1991**, *24*, 6182−6188.
(7) Winey, K. I.; Thomas, E. L.; Fetters, L. J. *J. Chem. Phys.* **1991**, *95* (12), 9367−9375.
(8) Winey, K. I.; Thomas, E. L.; Fetters, L. J. *Macromolecules* **1992**, *25*, 422−428.
(9) Koizumi, S.; Hasegawa, H.; Hashimoto, T. *Makromol. Chem., Macromol. Symp.* **1992**, *62*, 75−91.
(10) Lowenhaupt, B.; Hellmann, G. P. *Colloid Polym. Sci.* **1990**, *268*, 885.
(11) Lowenhaupt, B.; Hellmann, G. P. *Polymer* **1991**, *32*, 1065.
(12) Leibler, L.; Orland, H.; Wheeler, J. C. *J. Chem. Phys.* **1983**, *79* (7), 3550.
(13) Leibler, L.; Pincus, P. A. *Macromolecules* **1984**, *17*, 2922−2924.
(14) Leibler, L. *Makromol. Chem., Macromol. Symp.* **1988**, *16*, 1−17.
(15) Noolandi, J.; Hong, K. M. *Macromolecules* **1982**, *15*, 482−492; *Ibid.* **1984**, *17*, 1531−1537.
(16) Vilgis, T. A.; Noolandi, J. *Macromolecules* **1990**, *23*, 2941.
(17) Paul, D. R.; Newman, S. *Polymer Blends*; Academic Press: New York, 1978; Vol. 2, Chapter 12, p 42.
(18) Akiyama, M.; Jamieson, A. M. *Polymer* **1992**, *33*, 3582.
(19) Siqueira, D. F.; Nunes, S. P. *Polymer* **1994**, *35*, 490−495.
(20) Fowler, M. E.; Barlow, J. W.; Paul, D. R. *Polymer* **1987**, *28*, 2145−2149.
(21) Coleman, M. M.; Graf, J. F.; Painter, P. C. *Specific Interactions and Miscibility of Polymer Blends*; Technomic: Bassel, 1991; Chapter 2, p 113.
(22) Barlow, J. W.; Paul, D. R. *Polym. Eng. Sci.* **1987**, *20*, 1482−1494.
(23) Tucker, P. S.; Barlow, J. W.; Paul, D. R. *Macromolecules* **1988**, *21*, 2794−2800; **1990**, *23*, 745.
(24) Brown, H. R.; Deline, V. R.; Green, P. F. *Nature* **1989**, *341*, 221.
(25) Brown, H. R.; Char, K.; Deline, V. R. *Macromolecules* **1990**, *23*, 3383−3385.
(26) Braun, H.; Rudolf, B.; Cantow, H. J. *Polym. Bull.* **1994**, *32*, 241−248.
(27) Lowenhaupt, B.; Steurer, A.; Hellmann, G. P.; Gallot, Y. *Macromolecules* **1994**, *27*, 908−916.
(28) Flory, P. J. *Statistical Mechanics of Chain Molecules*; Hanser Publishers, Oxford Press, New York, 1989; Chapter 1, p 40.
(29) Cogan, K. A.; Gast, A. P. *Macromolecules* **1990**, *23*, 745.
(30) Perrin, P.; Purd'homme, R. E. *Macromolecules* **1994**, *27*, 1852−1860.
(31) Russell, T. P.; Anastasiadis, S. H.; Menelle, A.; Felcher, G. P.; Satija, S. K. *Macromolecules* **1991**, *24*, 1575.
(32) Leman, T. L. Unpublished result (1994).

MA951298U